

A 1961-2008 simulation of the Mediterranean Sea with NEMOMED8.

F. Sevault

V2.1 - September 2010

1 Presentation

This 1961-2008 simulation of the Mediterranean Sea with NEMOMED8 (Sevault et al. 2009) is computed with the longest and homogeneous series of atmospheric fluxes that we have at the moment, provided by the ARPEGE-Climate V4.6 model (Déqué and Piedelièvre 1995). It is slightly different from the one used by Beuvier et al. (2010), which was a 1961-2000 series computed with ARPEGE-Climate V4.5. One can refer to this article for all the setup of this new experiment, for the only differences are the atmospheric fluxes and a more recent version of the NEMOMED8 model. The atmospheric forcings come from a dynamical downscaling of the ERA40 fluxes (Simmons and Gibson 2000) followed by the ECMWF analysis taken at the ERA40 resolution (125 km instead of 55 km), using the spectral nudging technique. The large scales are driven by the observations, and the small scales can evolve freely, to take advantage of the 50 km resolution of the ARPEGE-Climate grid on Europe. The method to compute the atmospheric forcings is the same as in Beuvier et al. (2010) and Herrmann et al. (2010), but with another version of the atmospheric model. We call this series ARPERA-V2. The simulation begins after 15 years of spin-up, five with a 3D relaxation towards a climatology and ten with the same configuration. This document presents a set of results for this simulation, called NM8-ARPERA-V2.

2 The surface forcing

2.1 Atmospheric daily forcing

NEMOMED8 needs the momentum, the freshwater flux E-P (Evaporation minus Precipitation), the net and solar fluxes. They are interpolated from the ARPEGE-Climate grid to the NEMOMED8 grid with OASIS3 (Valcke 2006). The net flux is applied with a relaxation term using the observed sea surface temperature (SST) of ERA40. The E-P flux is corrected by a set of 12 mean monthly values, computed after a first simulation with a sea surface salinity relaxation to the climatology: we thus correct the too weak E-P flux of ARPERA-V2, knowing that it is also the case for the ERA40 series, in a way that let the sea surface salinity evolve more freely than with a classical relaxation. The yearly mean correction is equal to 0.2 mm/day, and the mean of E-P for ARPERA-V2 on the 1960-2008 period is equal to 2.16 mm/day before the correction.

2.2 Atlantic monthly forcing

The Atlantic part of the NEMOMED8 grid is used to simulate the circulation through the Gibraltar Strait, and thus to balance the heat and water budgets of the Mediterranean Sea. From 11°W to 7.5°W a 3D relaxation is applied to the temperature and salinity towards a dataset computed by Beuvier, which is a mixing of the Reynaud climatology (Reynaud et al. 1998) and the interannual monthly dataset of Daget (Daget et al. 2009). This dataset stops in 2005, this year is kept for the three last years of the simulation.

2.3 Monthly river runoffs

The river runoffs are explicitly added to the freshwater flux. 33 river mouths are introduced in the model and the dataset is computed by Beuvier, which is a mixing of the RivDis database (Vörösmarty et al. 1996) and the Ludwig et al. (2009) database. The dataset stops in 2000, this year is kept for the last years of the simulation.

2.4 Black Sea input

The Black Sea isn't included in the NEMOMED8 grid, but its input of poorly salted water is essential for the Aegean Sea. It is introduced as a river runoff, with interannual monthly cycles coming from Stanev et al. (2000) and Stanev and Peneva (2002). The interannual data we use stop in 1997, this year is kept for the last years of the simulation.

3 Results

The annual means are given from 1961 (year 0) to 2008 (year 47), and computed on the whole Mediterranean basin when the basin isn't explicitly named.

3.1 Surface

3.1.1 Sea surface temperature (SST) and salinity (SSS)

Figure 1 shows the yearly averages on the Mediterranean Sea, compared to the observed SST dataset used for the relaxation (ERA40) and the climatology of M. Rixen (from the NURC, Rixen et al. 2005). Table 1 gives some statistical values.

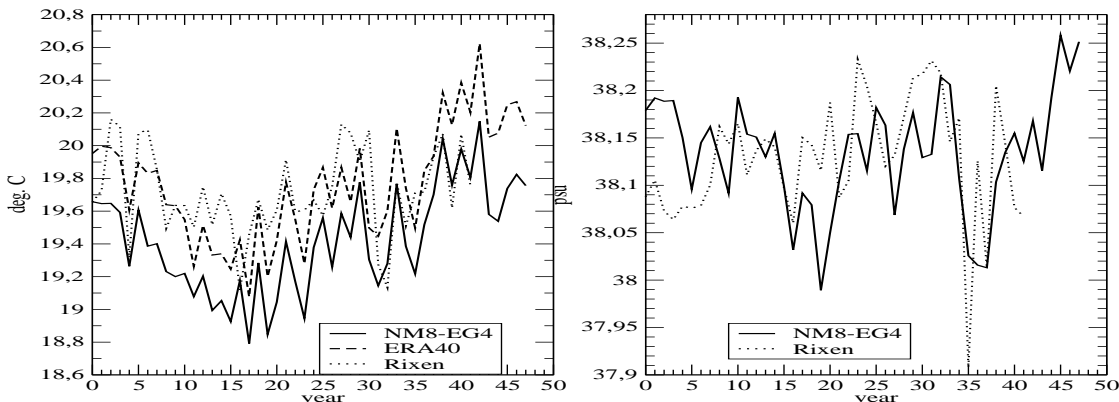


Figure 1: Yearly means of SST (left) and SSS (right) on the Mediterranean basin

	NM8-ARPERA-V2 (1961-2008)	ERA40 (1961-2008)	Rixen (1961-2002)
SST mean in °C (stdev) (correlation)	19.42 (0.32)	19.77 (0.35) (0.98)	19.71 (0.27) (0.60)
SSS mean in psu (stdev) (correlation)	38.13 (0.06)		38.13 (0.06) (0.36)

Table 1: Mean and standard deviation of SST and SSS, correlation with NM8-ARPERA-V2 on the same period (timeseries without trends)

3.1.2 Heat and water fluxes

The net heat flux (q_{tot}) received by the ocean surface is the sum of the ARPERA-V2 net surface heat flux (Q_{tot} ARPERA-V2) and the relaxation term to the observed SST (q_{rp}).

The water flux (emp) received by the ocean surface is equal to $E-P-R+erp$, where $E-P$ is the Evaporation-Precipitation term of ARPERA-V2 ($E-P$ ARPERA-V2), R is the river runoff coming from the database, and erp is the correction term explained in §2.1.

Figure 2 shows the yearly averages of the different fluxes, and table 2 gives the means and standard deviations.

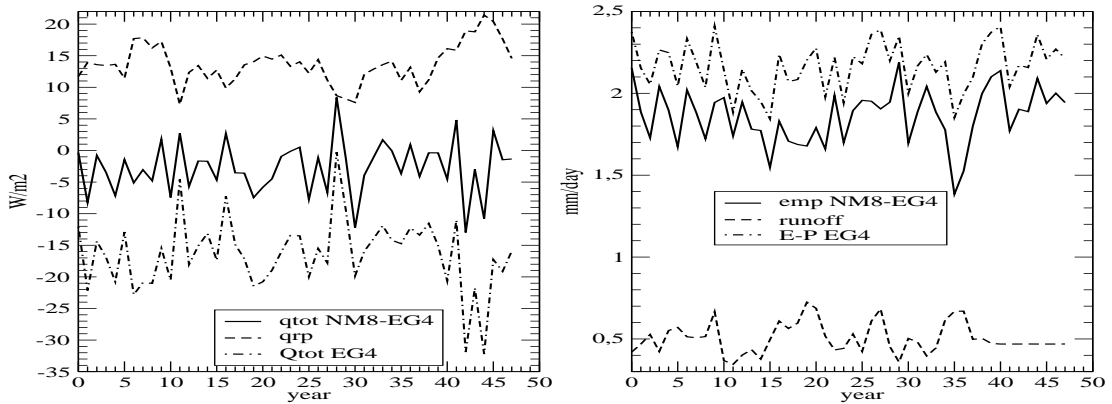


Figure 2: Yearly means of the surface heat (left) and water fluxes (right)

(1961-2008)	q_{tot} NM8-ARPERA-V2	q_{rp}	Q_{tot} ARPERA-V2	emp NM8-ARPERA-V2	runoff	$E-P$ ARPERA-V2
mean	-2.74 W/m^2	13.66 W/m^2	-16.40 W/m^2	1.86 mm/day	0.50 mm/day	2.16 mm/day
stdev	4.20	3.13	5.64	0.17	0.09	0.15

Table 2: Annual means and standard deviation of the surface fluxes

3.1.3 Mean seasonal surface salinity and temperature

Figure 3 and figure 4 show the surface salinity and temperature averaged for each season January-February-March, April-May-June, July-August-September, and October-November-December, of the whole 1961-2008 period.

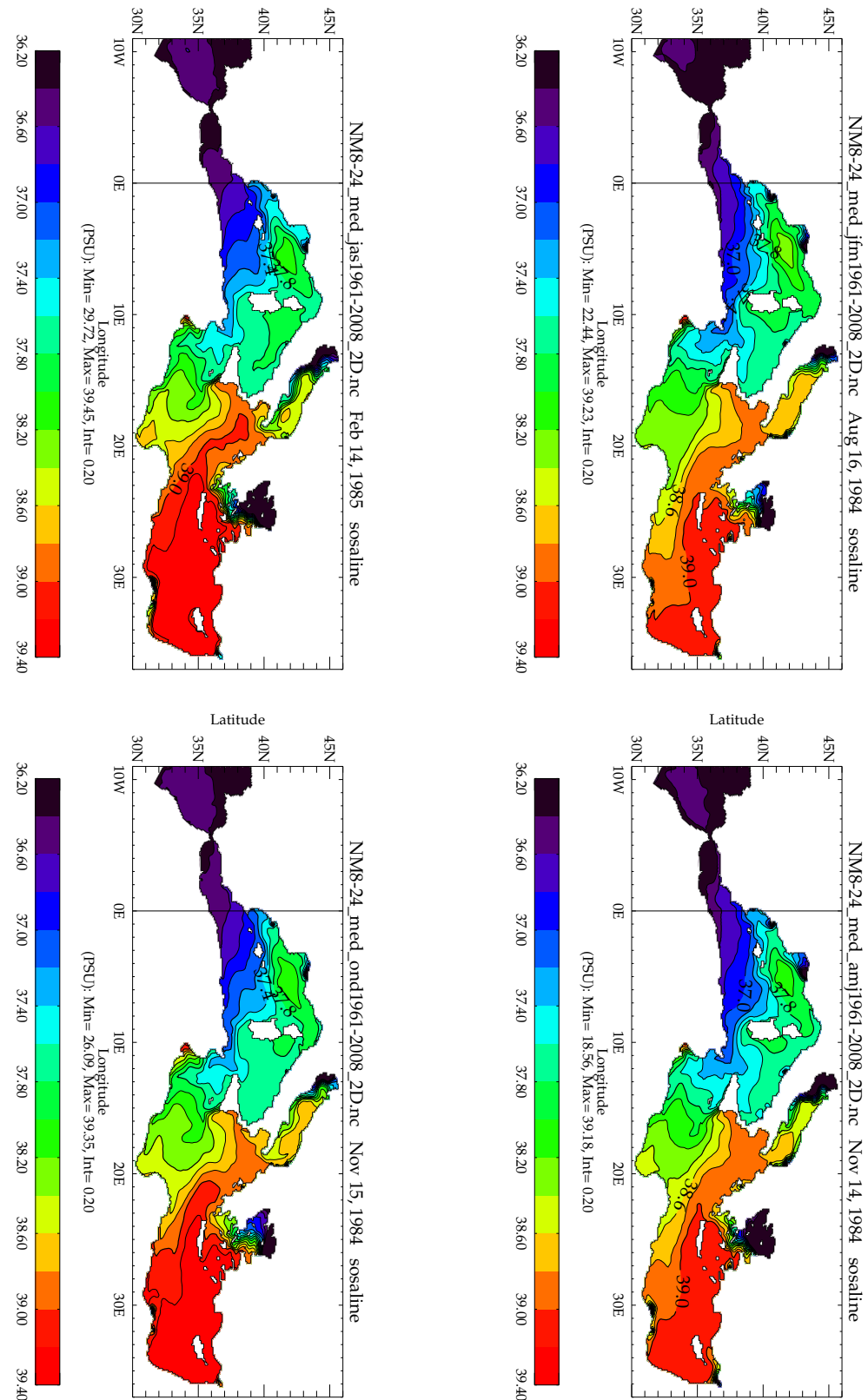


Figure 3: Seasonal 1961-2008 surface salinity, JFM top left, AMJ top right, JAS bottom left, and OND bottom right.

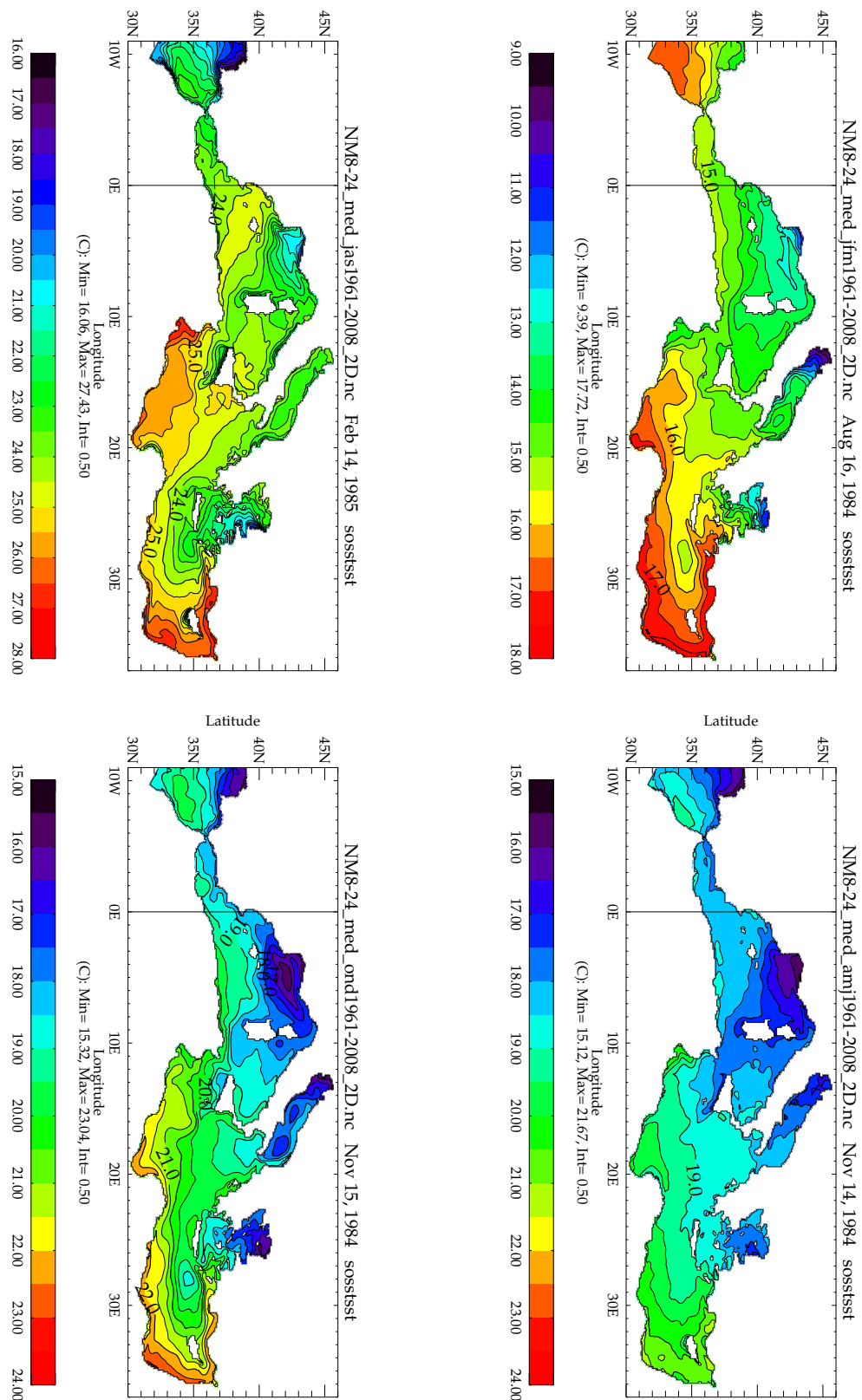


Figure 4: Seasonal 1961-2008 surface temperature, JFM top left, AMJ top right, JAS bottom left, and OND bottom right.

3.1.4 Sea surface height and circulation

Figure 5 shows the 1961-2008 sea surface height (m) and circulation (m/s).

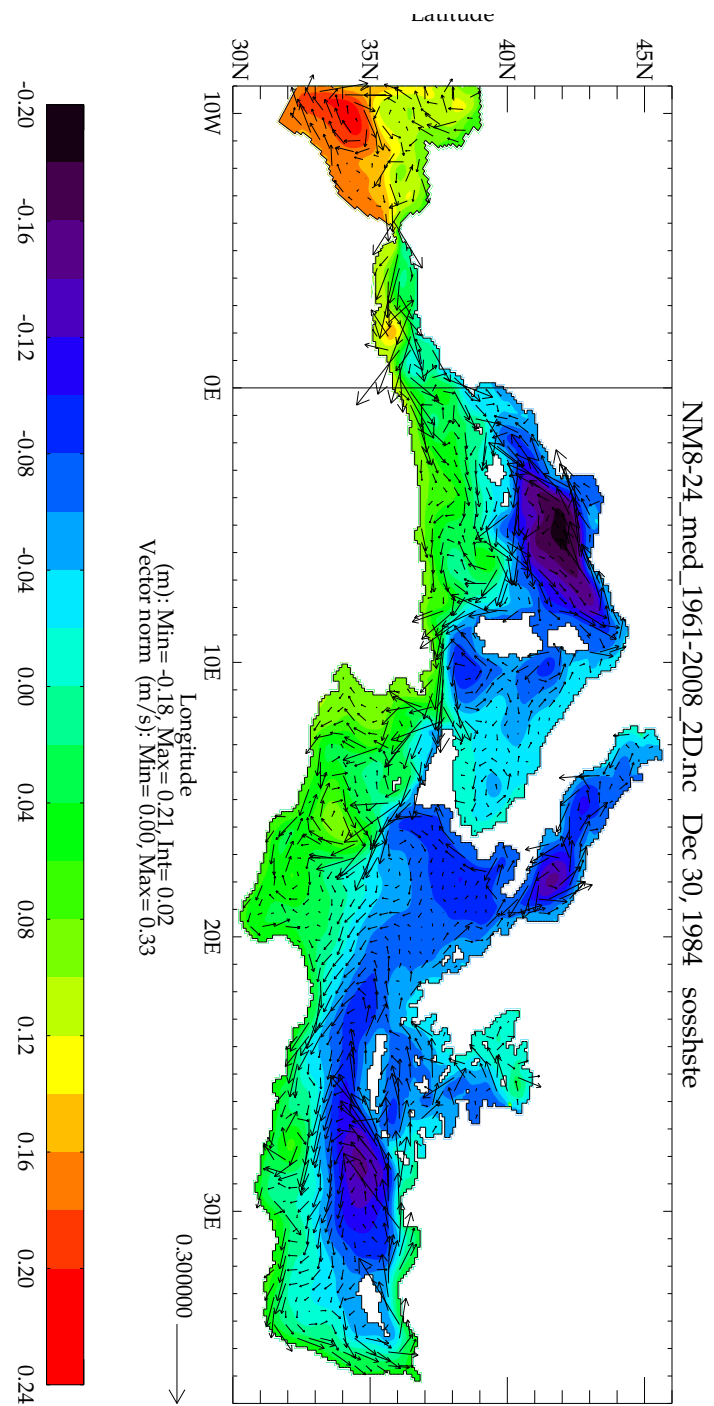


Figure 5: 1961-2008 sea surface height computed with the steric effect and circulation

3.1.5 Annual sea surface height and column density

We compare the column density of the Mediterranean (MED) and the Western (MEDW) basins averaged yearly with the Rixen climatology on the 1961-2002 period (fig. 6, 1st row). Figure 6 (second row) shows the yearly averaged sea surface height (ssh), and computed with the steric effect (sshste).

Table 3 gives the average, standard deviation, and correlation of the two sets of column density. The correlations are computed on timeseries without trends.

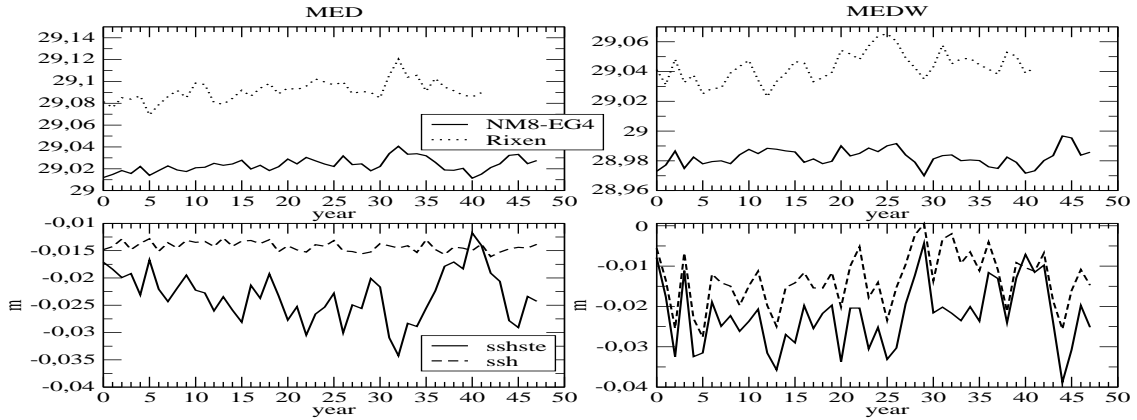


Figure 6: Yearly column density (top) and sea surface height (bottom) for the MED (left) and MEDW (right) basins

Column density	NM8-ARPERA-V2 (1961-2008)	Rixen (1961-2002)	Correlation (1961-2002)
MED (stdev)	29.02 (0.01)	29.09 (0.01)	0.67
MEDW (stdev)	28.98 (0.01)	29.04 (0.01)	0.60

Table 3: Mean and standard deviation of the yearly averaged column density, correlation on the 1961-2002 period (timeseries without trends)

3.2 Thermal and salinity content

For the whole basin (MED, fig. 7) and the sub-basins MEDW (fig. 8), MEDE (Eastern basin without the Adriatic and Aegean Seas, fig. 9) ADRI (Adriatic Sea, fig. 10) and EGEE (Aegean Sea, fig. 11), we present the yearly column temperature and salinity of NM8-ARPERA-V2 compared to the Rixen climatology (average plus/minus one standard deviation).

Table 4 gives the averages, standard deviations and correlations of the temperature and salinity (line 0-b, timeseries without trends).

	NM8-ARPERA-V2	Rixen clim	Correlation	NM8-ARPERA-V2	Rixen clim	Correlation
	T3D				S3D	
	MED				MED	
0-b	13.83 (0.06)	13.69 (0.03)	0.71	38.65 (0.02)	38.62 (0.01)	0.24
0-150m	16.32 (0.22)	16.30 (0.15)	0.78	38.31 (0.03)	38.35 (0.03)	0.06
150-600m	14.33 (0.07)	14.07 (0.08)	0.76	38.80 (0.01)	38.71 (0.02)	0.11
600m-b	13.39 (0.06)	13.25 (0.02)	0.42	38.66 (0.02)	38.62 (0.01)	0.45
	MEDW				MEDW	
0-b	13.38 (0.07)	13.17 (0.03)	0.67	38.44 (0.02)	38.41 (0.01)	-0.06
0-150m	15.28 (0.23)	15.11 (0.16)	0.78	37.65 (0.04)	37.87 (0.06)	0.40
150-600m	13.87 (0.09)	13.41 (0.07)	0.82	38.61 (0.03)	38.48 (0.02)	-0.15
600m-b	13.01 (0.06)	12.88 (0.02)	0.17	38.49 (0.02)	38.45 (0.01)	-0.05
	MEDE				MEDE	
0-b	14.06 (0.06)	14.01 (0.03)	0.72	38.77 (0.02)	38.74 (0.01)	0.31
0-150m	17.04 (0.26)	17.07 (0.20)	0.72	38.66 (0.03)	38.63 (0.03)	0.04
150-600m	14.59 (0.08)	14.49 (0.10)	0.80	38.90 (0.01)	38.85 (0.02)	0.31
600m-b	13.60 (0.07)	13.49 (0.02)	0.35	38.75 (0.02)	38.73 (0.01)	0.41
	EGEE				EGEE	
0-b	15.09 (0.17)	14.71 (0.13)	0.82	38.91 (0.04)	38.83 (0.04)	0.38
0-150m	16.41 (0.36)	16.59 (0.34)	0.79	38.74 (0.11)	38.74 (0.08)	0.34
150-600m	14.76 (0.20)	14.47 (0.16)	0.66	38.98 (0.04)	38.90 (0.04)	0.40
600m-b	14.19 (0.16)	13.69 (0.06)	0.27	38.97 (0.07)	38.81 (0.03)	-0.01
	ADRI				ADRI	
0-b	14.40 (0.21)	14.20 (0.18)	0.28	38.71 (0.08)	38.51 (0.04)	0.07
0-150m	15.33 (0.30)	15.16 (0.30)	0.49	38.59 (0.15)	38.27 (0.07)	0.35
150-600m	13.95 (0.25)	13.78 (0.16)	-0.14	38.78 (0.09)	38.69 (0.04)	-0.32
600m-b	13.66 (0.16)	13.25 (0.11)	0.08	38.79 (0.06)	38.65 (0.03)	-0.43

Table 4: Averages, standard deviations and correlations of the temperature (left) and salinity (right), b for bottom. The correlations are computed on timeseries without trends and on the 1961-2002 period.

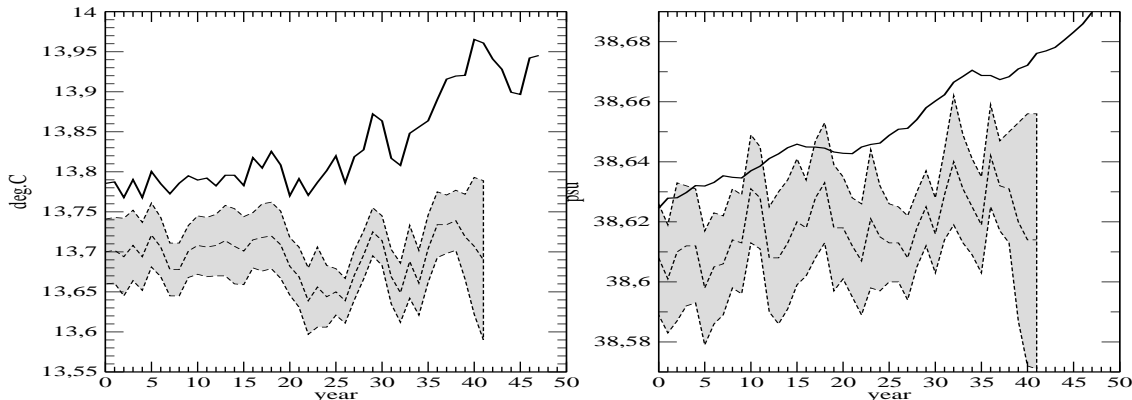


Figure 7: MED, yearly mean of the column temperature (left) and salinity (right), NM8-ARPERA-V2 in black, Rixen climatology in grey

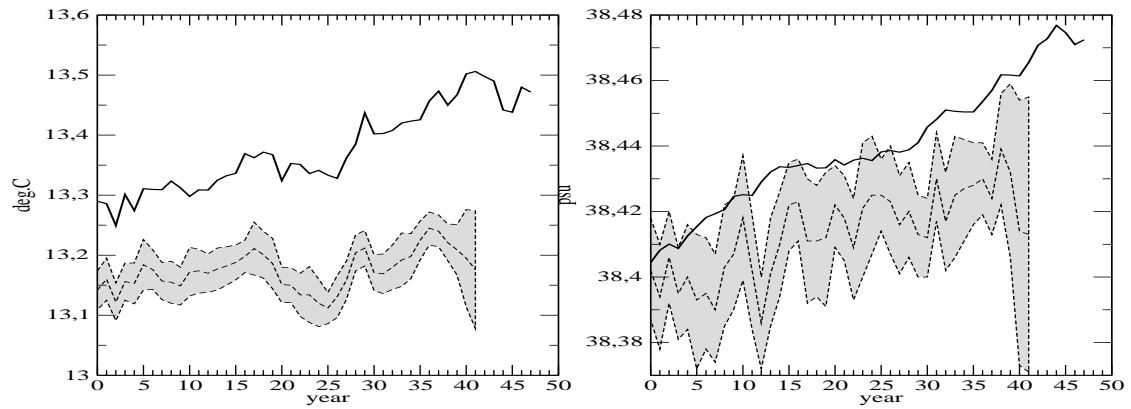


Figure 8: MEDW, same as fig. 7

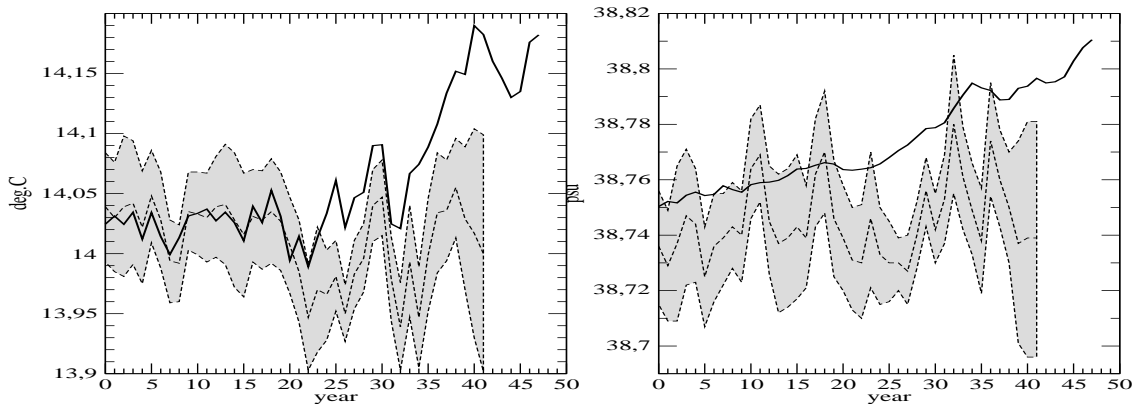


Figure 9: MEDE, same as fig. 7

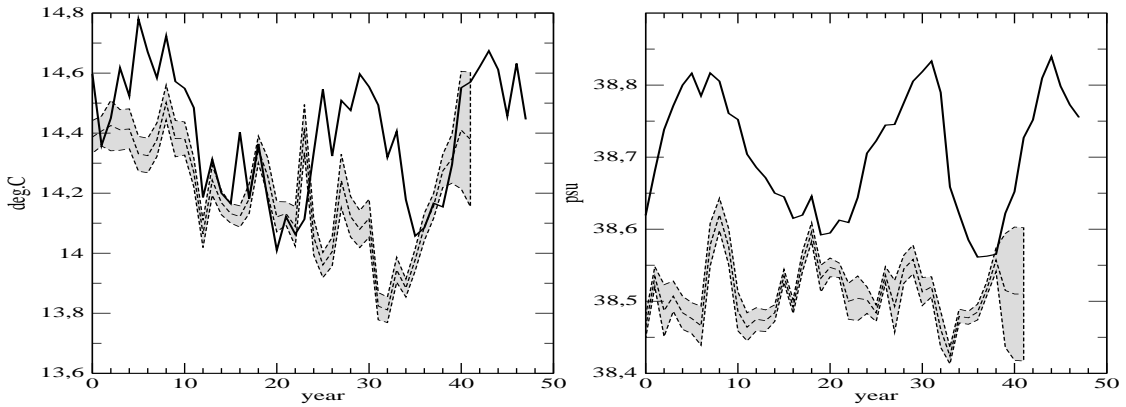


Figure 10: ADRI, same as fig. 7

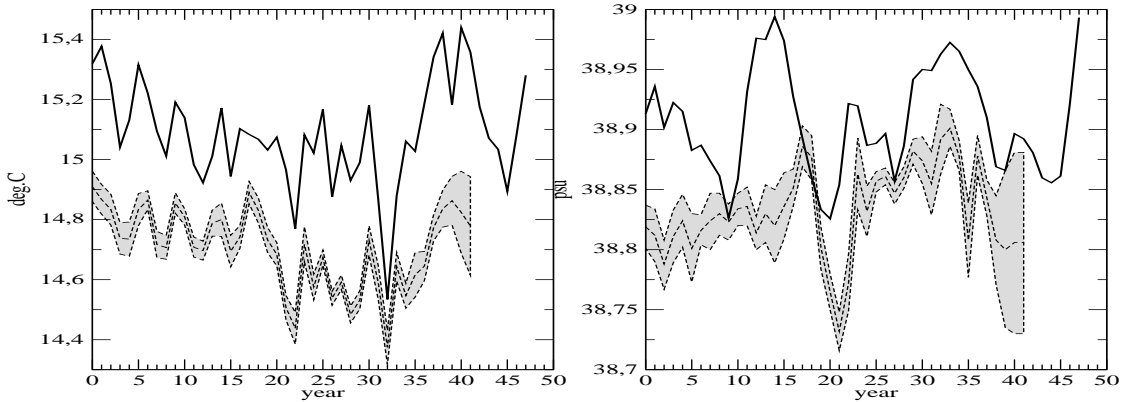


Figure 11: EGEE, same as fig. 7

3.3 Thermal and salinity content for the column divided in three layers: 0-150m, 150-600m and 600m-bottom.

The thermal and salinity content for the three layers are computed for the MED (fig. 12), MEDW (fig. 13), MEDE (fig. 14), ADRI (fig. 15) and EGEE (fig. 16) basins.

Table 4 gives the averages, standard deviations and correlations of the temperature and salinity. The correlations are computed on timeseries without trends.

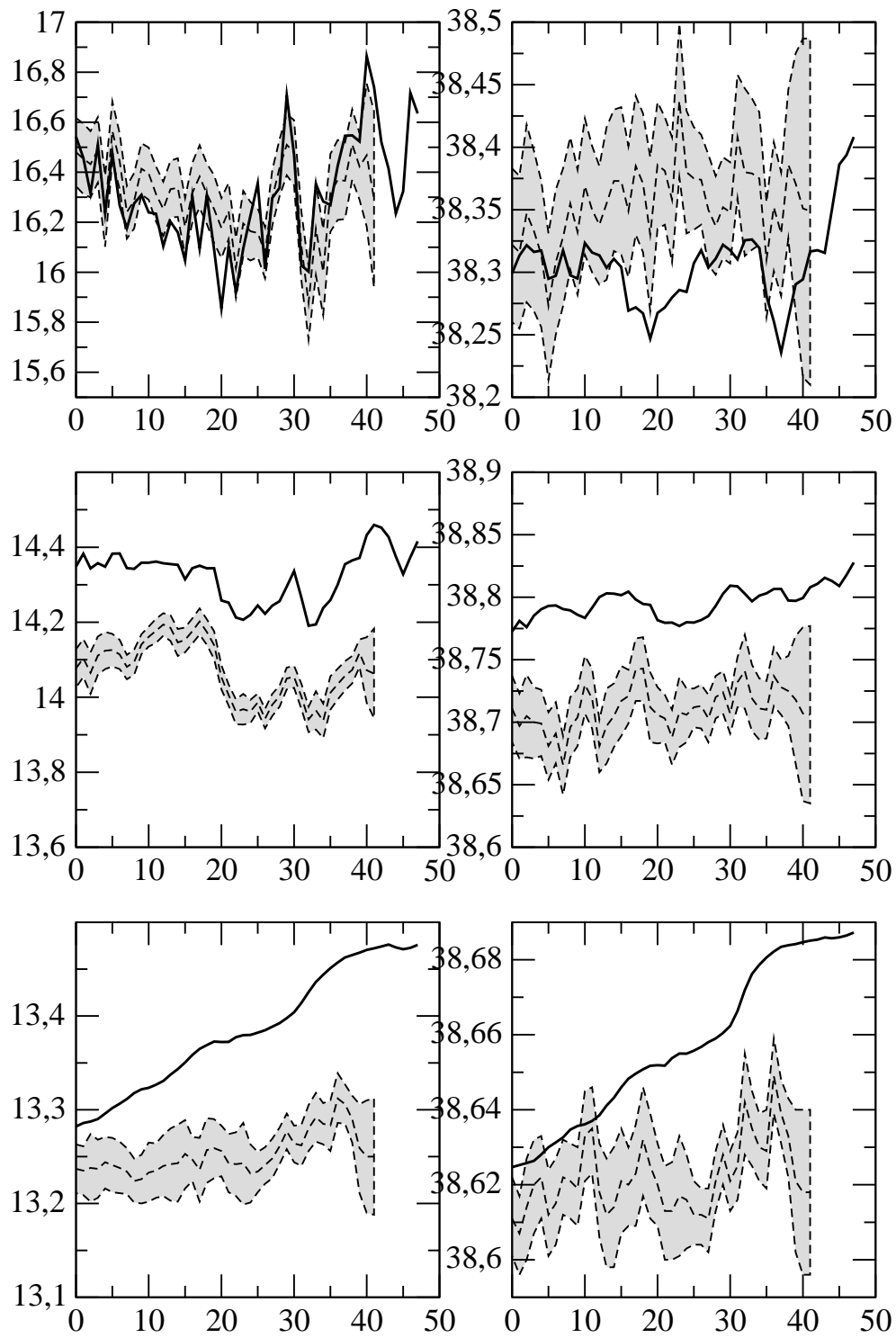


Figure 12: MED, yearly means of the column temperature (left) and salinity (right) for the 0-150m (top), 150-600m (middle) and 600m-bottom (bottom) layers, NM8-ARPERA-V2 in black, Rixen climatology in grey.

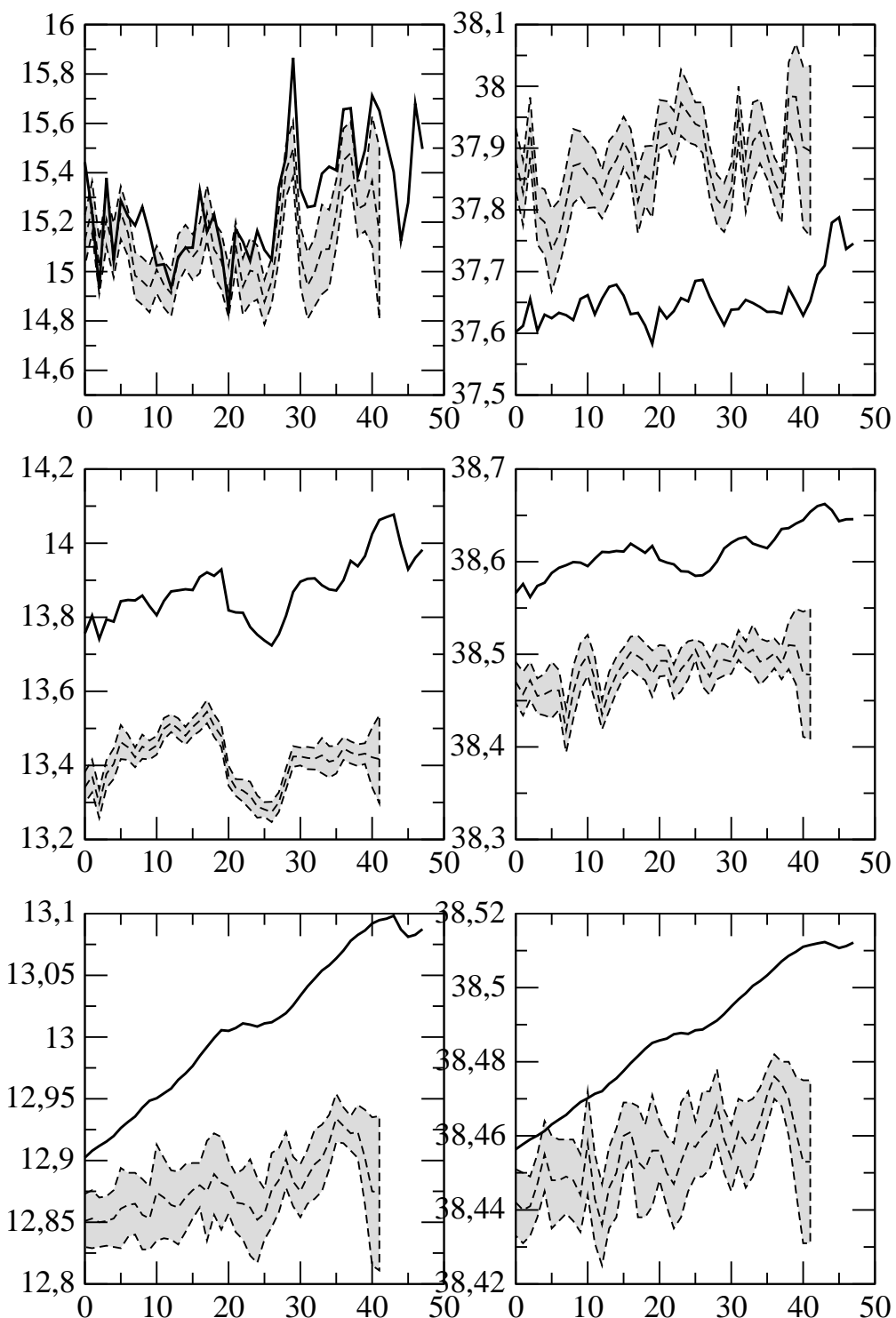


Figure 13: MEDW, same as fig. 12

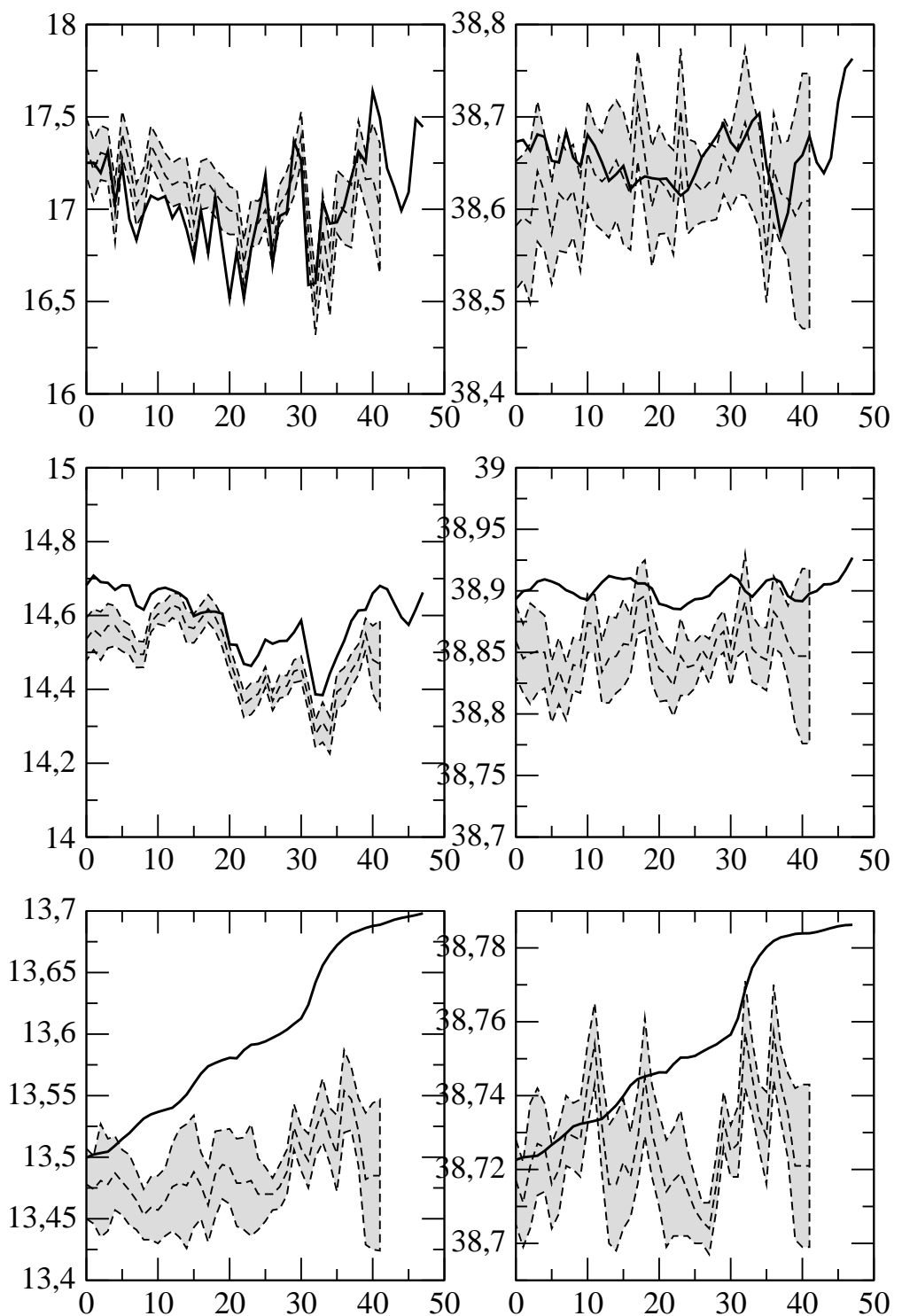


Figure 14: MEDE, same as fig. 12

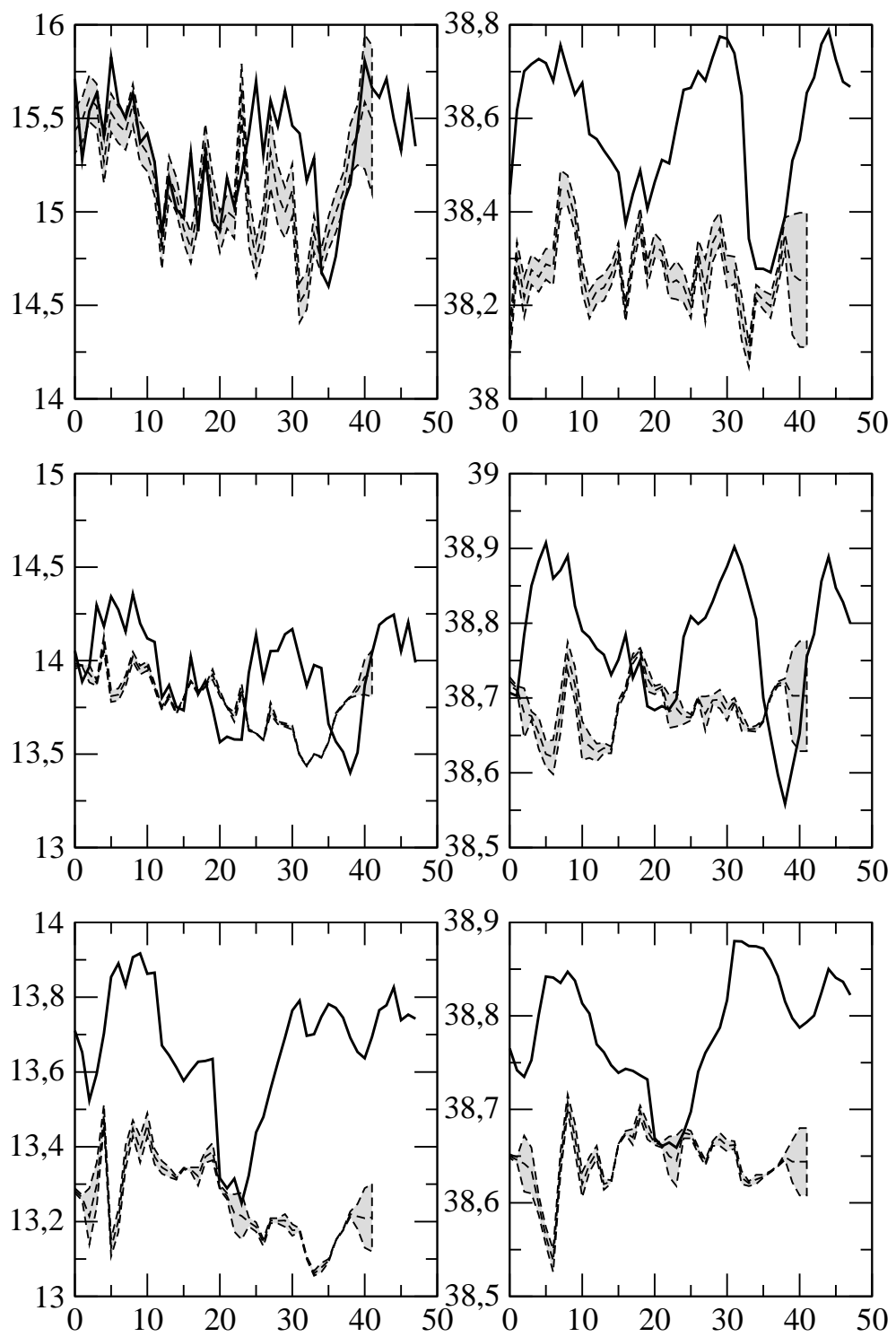


Figure 15: ADRI, same as fig. 12

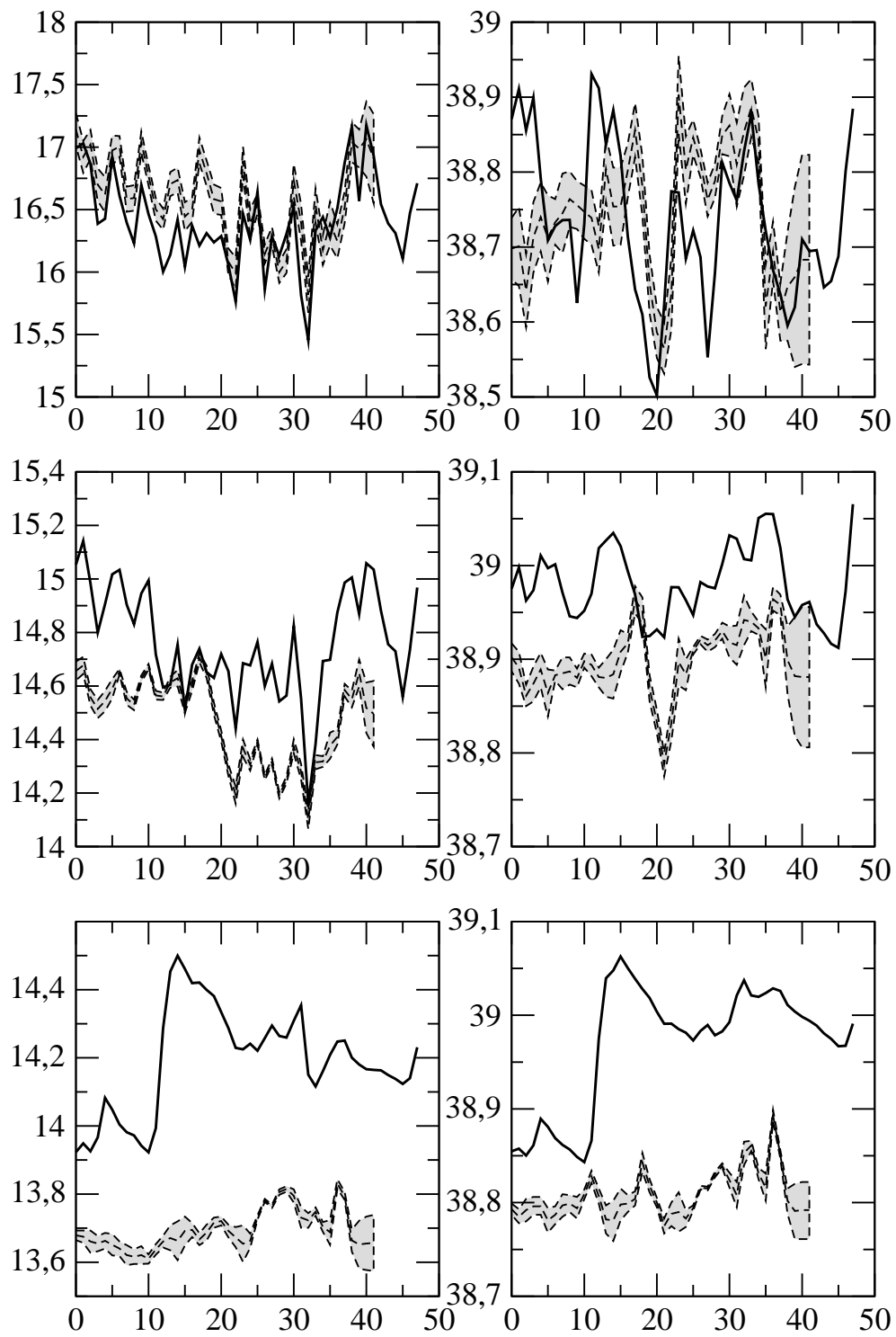


Figure 16: EGEE, same as fig. 12

3.4 Mixed layer depth

3.4.1 Mean 1961-2008 winter mixed layer depth (January-February-March)

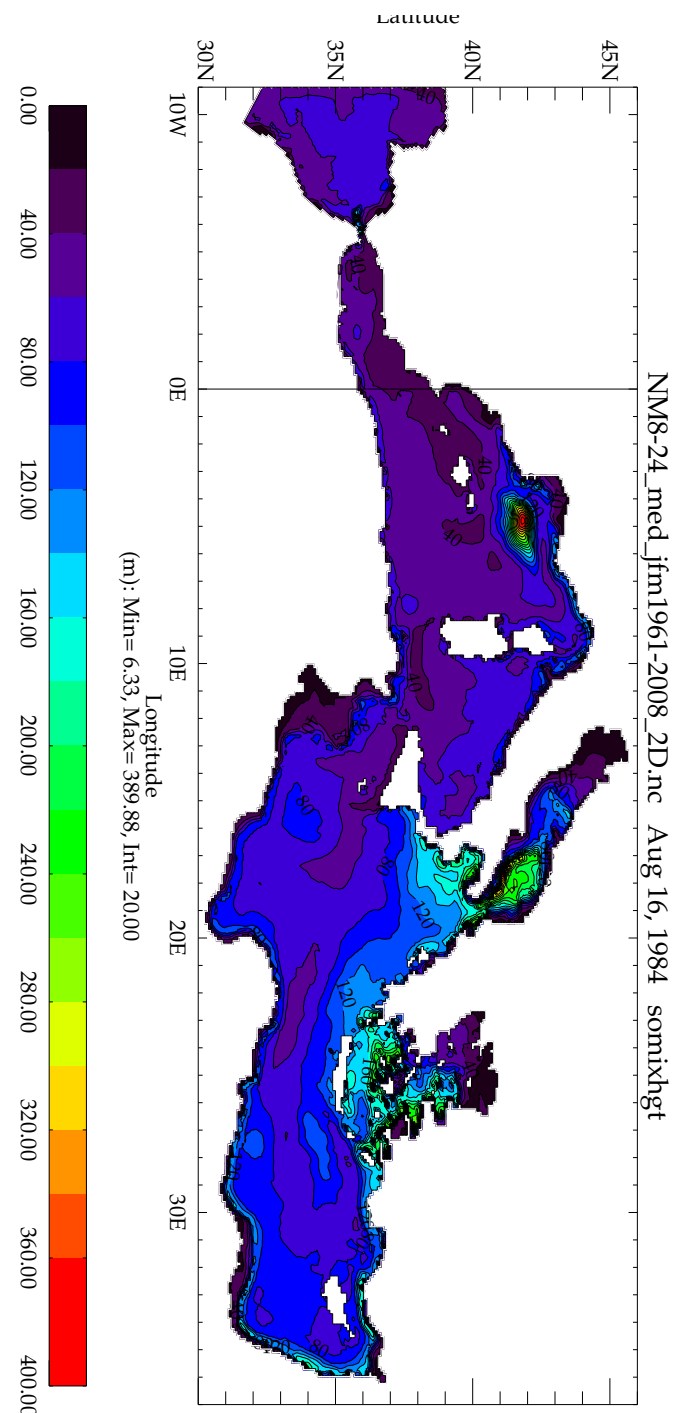


Figure 17: 1961-2008 JFM mixed layer depth (m)

3.4.2 Maximum daily mixed layer depth

The maximum daily mixed layer depth is computed each year for the Adriatic (ADRI), Aegean (EGEE), Levantine (LEVA) and Gulf of Lions (LION4) basins (fig. 18). For the latter the red stars show the maximum depth read in Mertens and Schott (1998), and the 2005 deep convection.

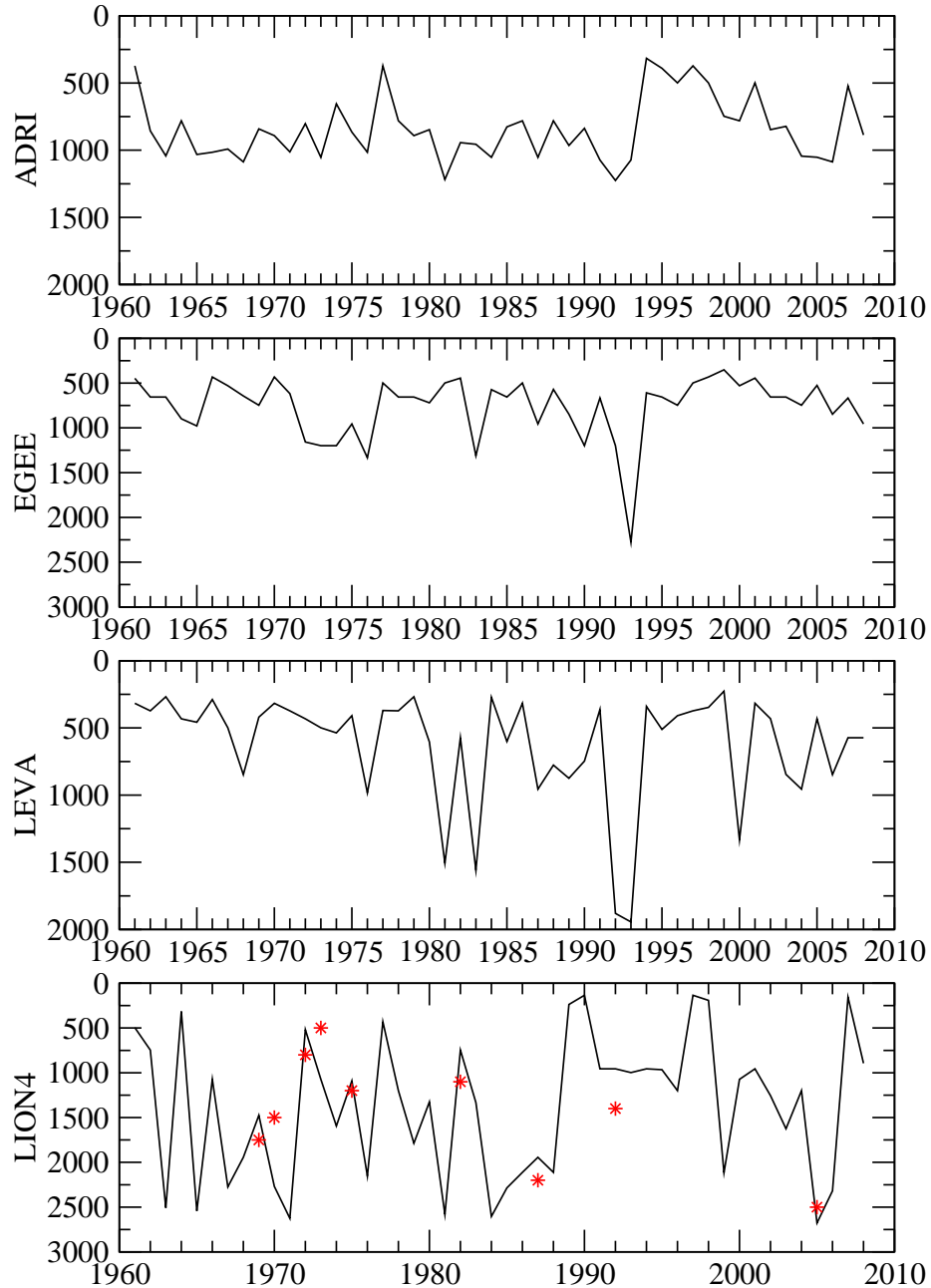


Figure 18: Maximum daily mixed layer depth (m) each year

3.5 Zonal and meridional overturning functions

The overturning function shows in a vertical plan the zonal (or meridional) circulation integrated along the latitudes (or the longitudes) of the basin. We will show the result on the whole 1961-2008 period, and divided in three periods, 1961-1990, 1991-1994, and 1995-2008, so that the Eastern Mediterranean Transient period can be analysed.

The zonal overturning function is computed on the whole Mediterranean basin (MED). The meridional overturning function is computed for the MEDW $>38^{\circ}\text{N}$ basin, that is for the latitudes greater than 38°N , and for the Adri-Ionian basin, gathering the Adriatic and Ionian Seas for latitudes greater than 37°N .

Figures 19 to 30 show these functions on the different periods and basins.

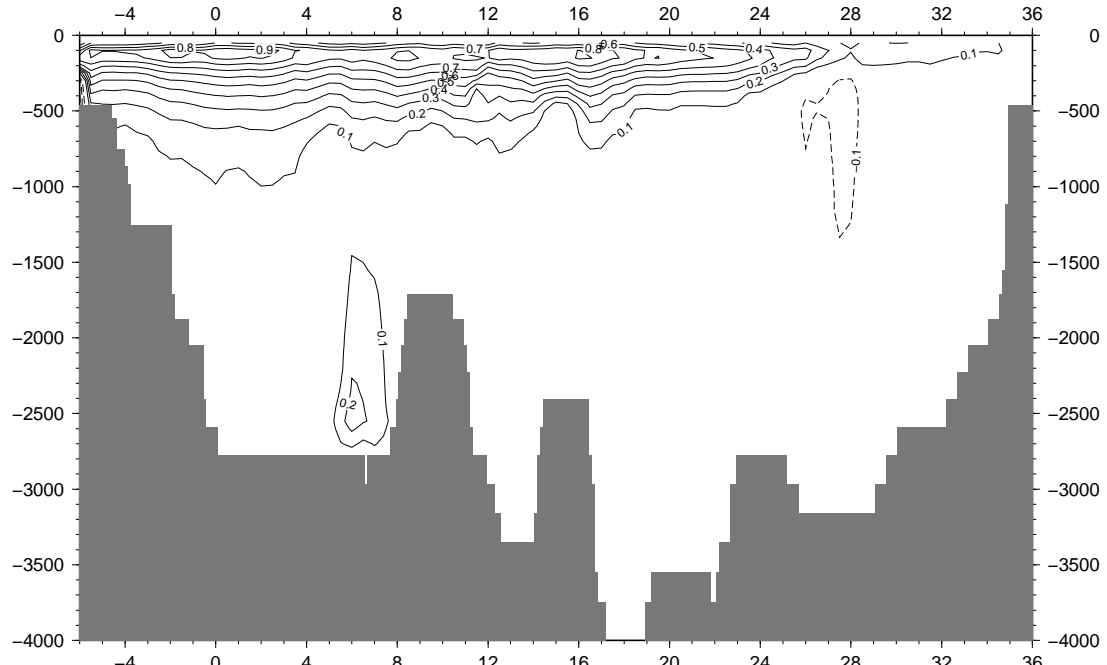


Figure 19: 1961-2008 zonal overturning function on the MED basin; the x-axis shows the longitudes.

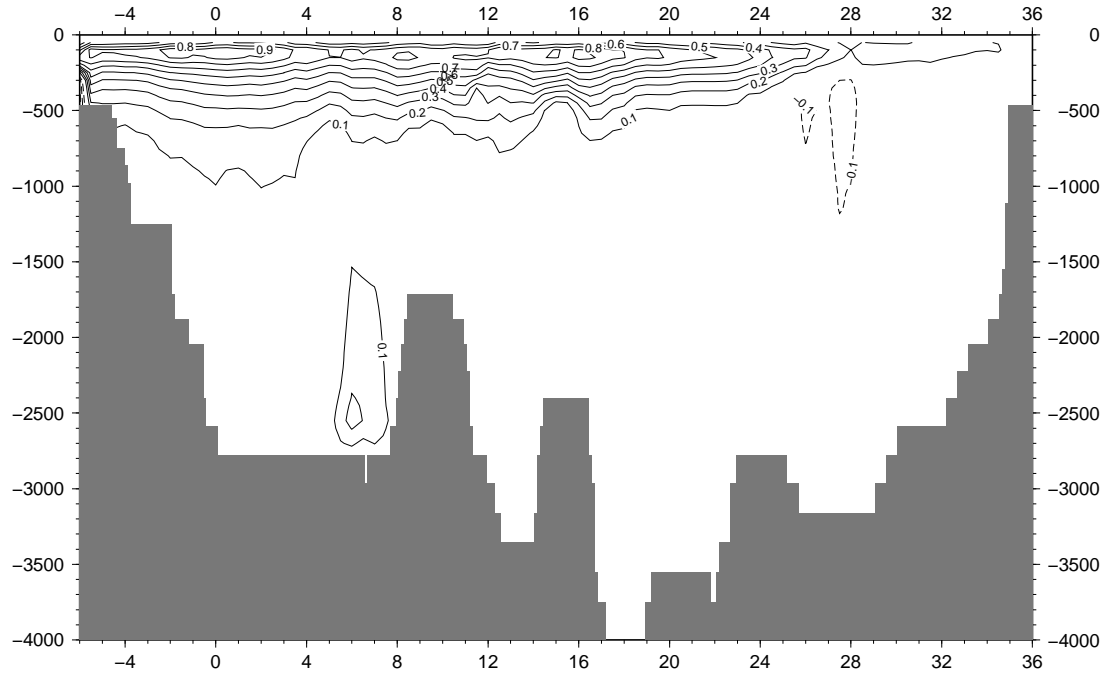


Figure 20: 1961-1990 zonal overturning function on the MED basin; the x-axis shows the longitudes.

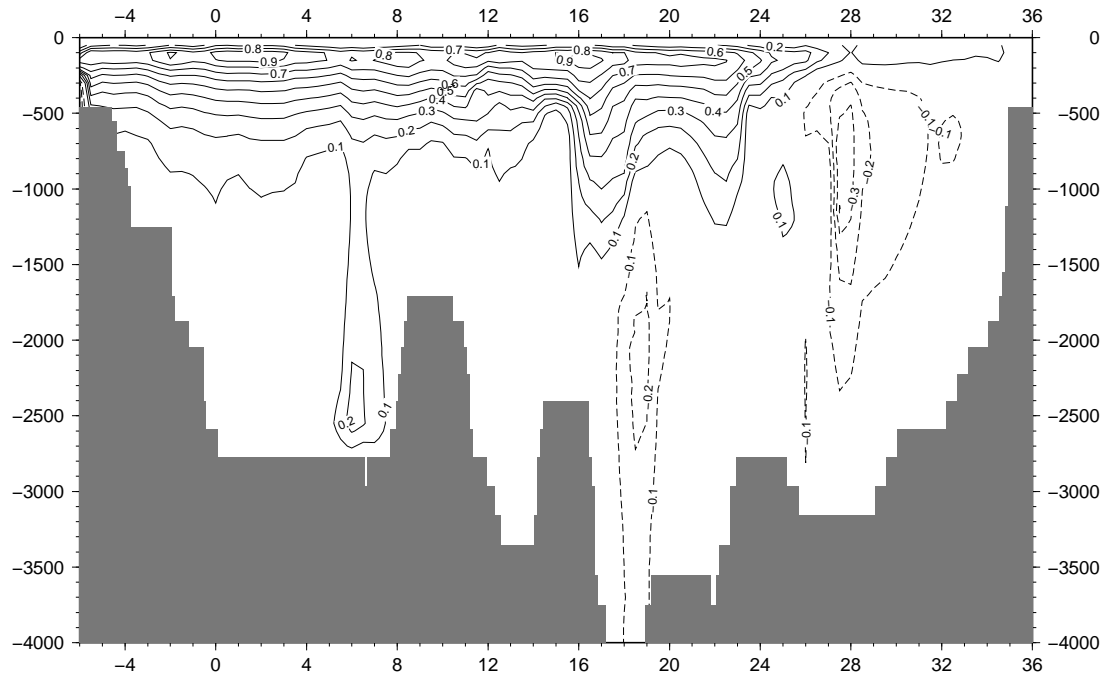


Figure 21: 1991-1994 zonal overturning function on the MED basin; the x-axis shows the longitudes.

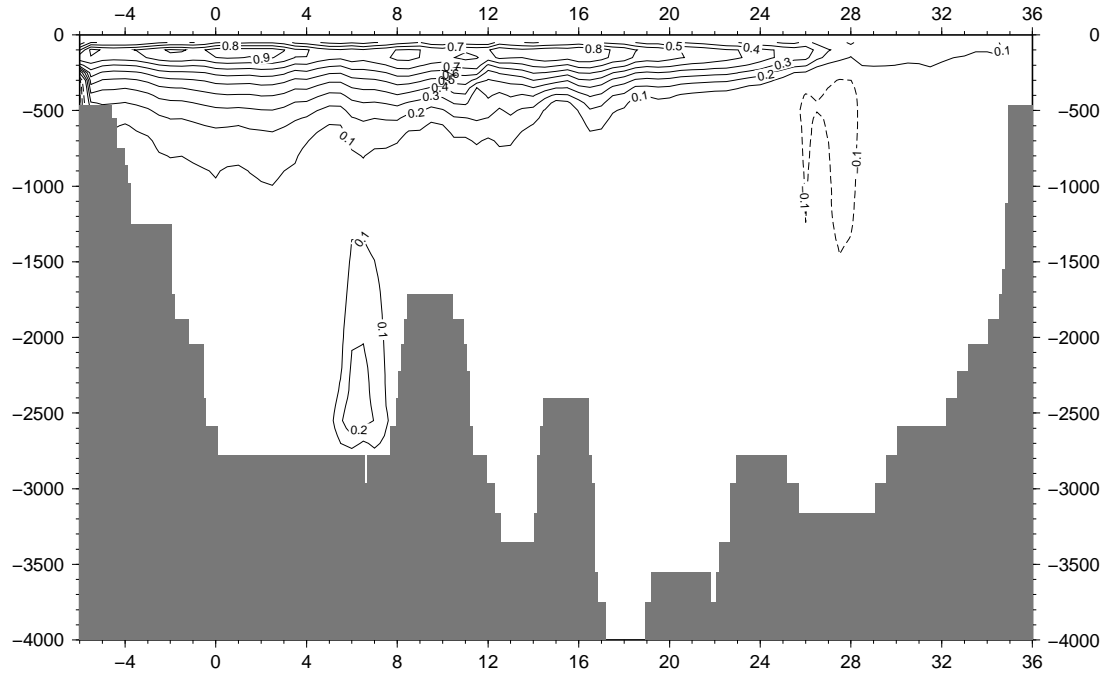


Figure 22: 1995-2008 zonal overturning function on the MED basin; the x-axis shows the longitudes.

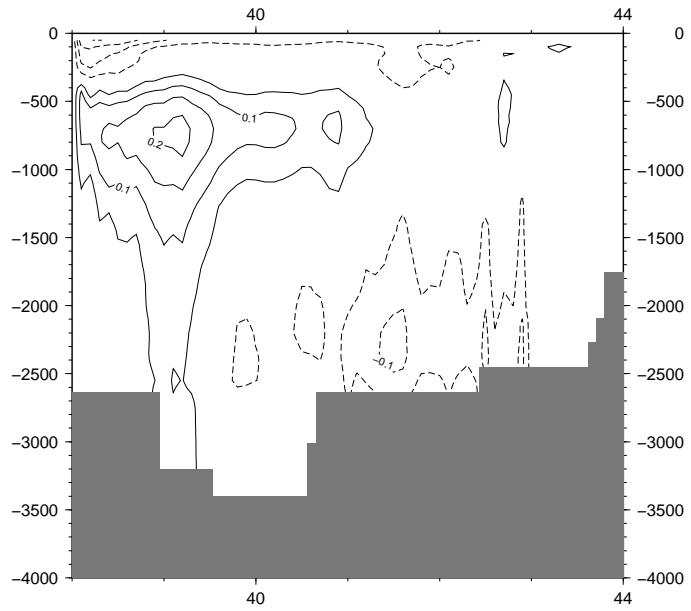


Figure 23: 1961-2008 meridional overturning function on the MEDW $> 38^\circ\text{N}$ basin; the x-axis shows the latitudes.

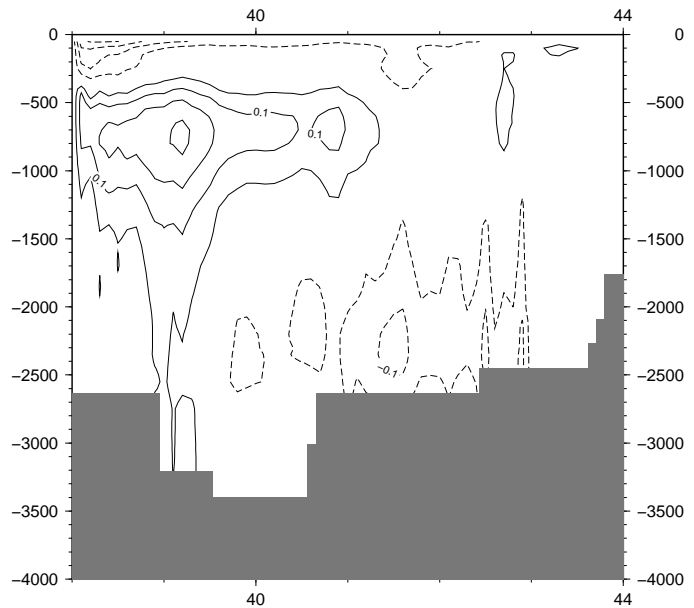


Figure 24: 1961-1990 meridional overturning function on the MEDW $>38^{\circ}\text{N}$ basin; the x-axis shows the latitudes.

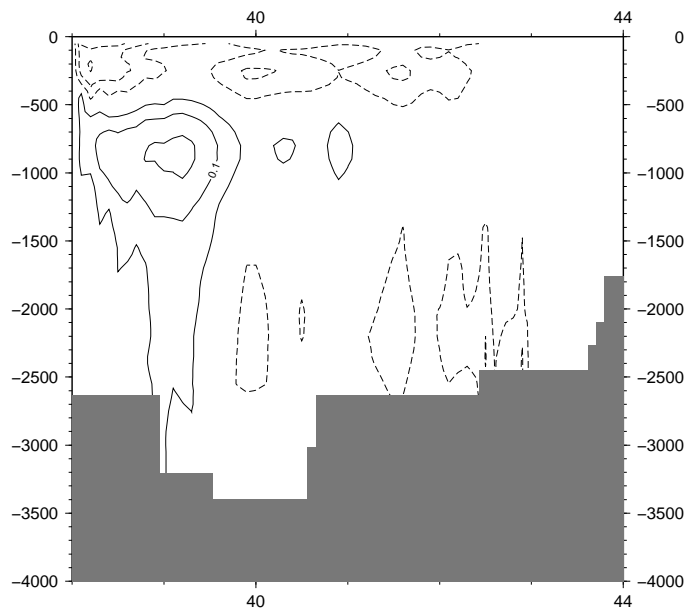


Figure 25: 1991-1994 meridional overturning function on the MEDW $>38^{\circ}\text{N}$ basin; the x-axis shows the latitudes.

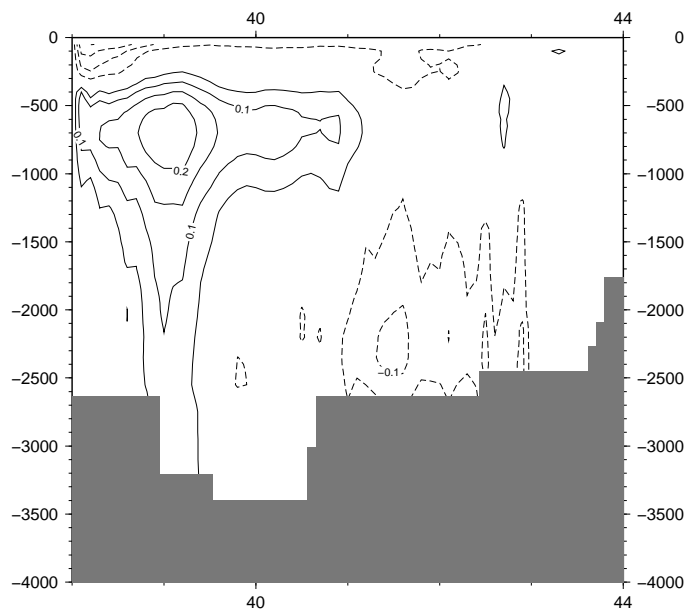


Figure 26: 1995-2008 meridional overturning function on the MEDW $>38^{\circ}\text{N}$ basin; the x-axis shows the latitudes.

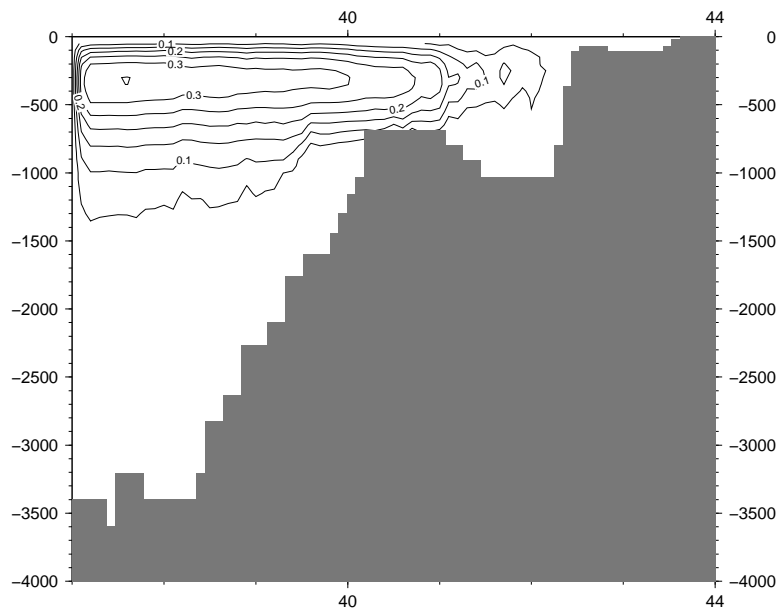


Figure 27: 1961-2008 meridional overturning function on the Adri-Ionian basin; the x-axis shows the latitudes.

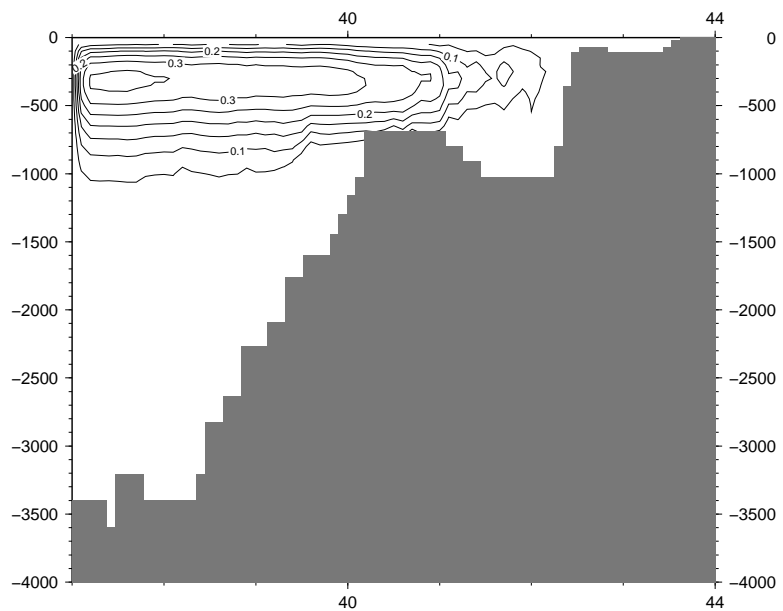


Figure 28: 1961-1990 meridional overturning function on the Adri-Ionian basin; the x-axis shows the latitudes.

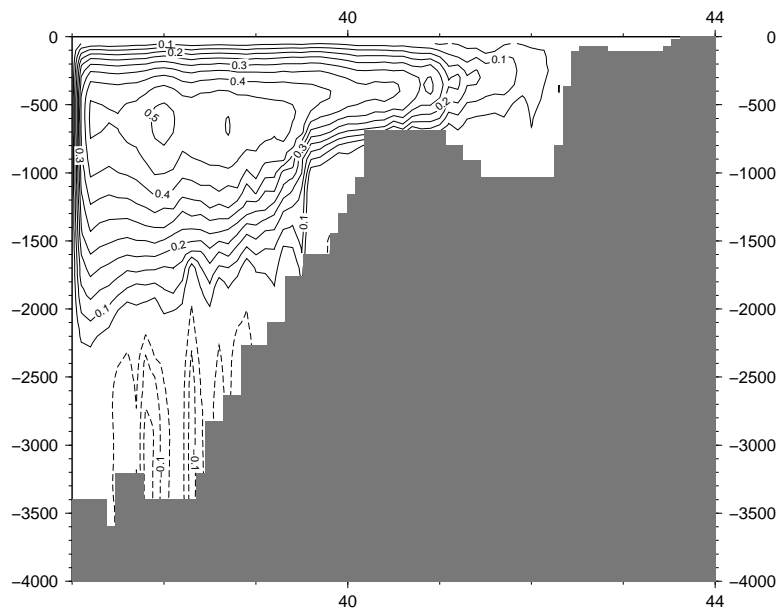


Figure 29: 1991-1994 meridional overturning function on the Adri-Ionian basin; the x-axis shows the latitudes.

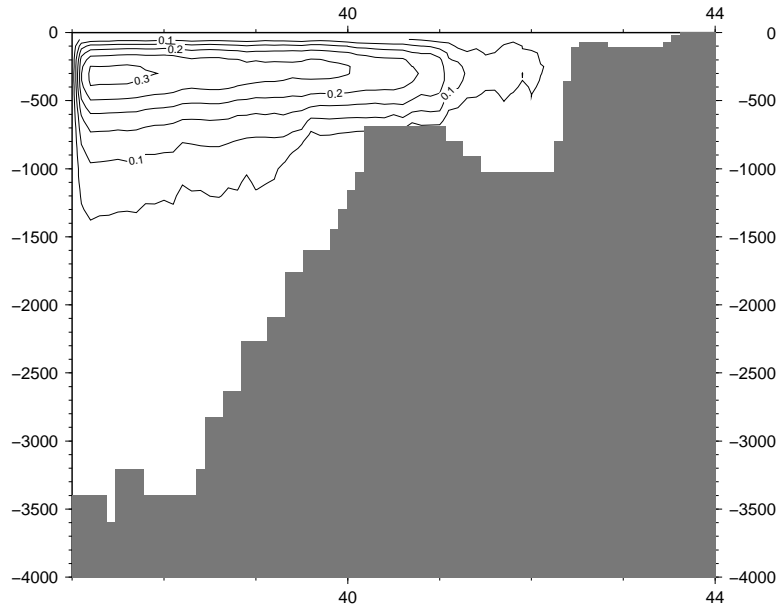


Figure 30: 1995-2008 meridional overturning function on the Adri-Ionian basin; the x-axis shows the latitudes.

3.6 Annual transport at the Gibraltar strait

The average 1961-2008 net transport of NM8-ARPERA-V2 is 0.05 Sv, the incoming 0.86 Sv and the outgoing -0.81 Sv. See figure 31 for the evolution.

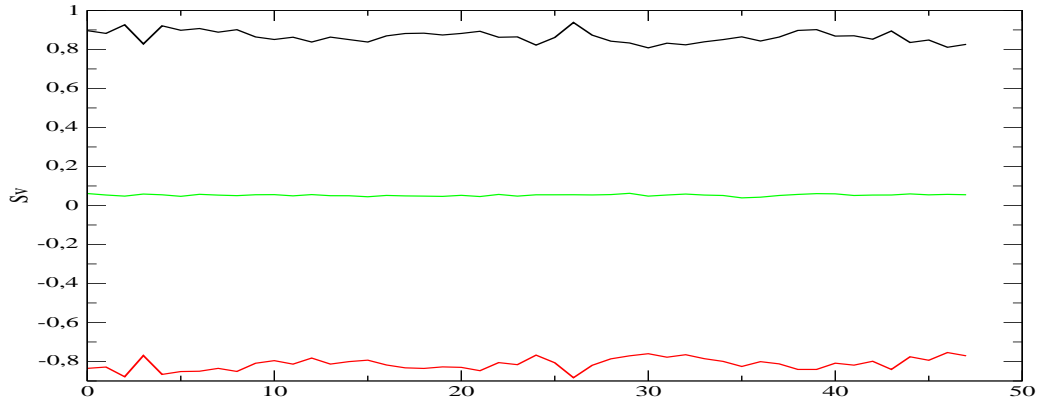


Figure 31: Annual transport at the Gibraltar Strait 1961-2008

3.7 Monthly volume of water with density criteria

We compute the monthly volume of water which density is greater than 29.1, 29.2 and 29.3 in four subbasins (figure 32).

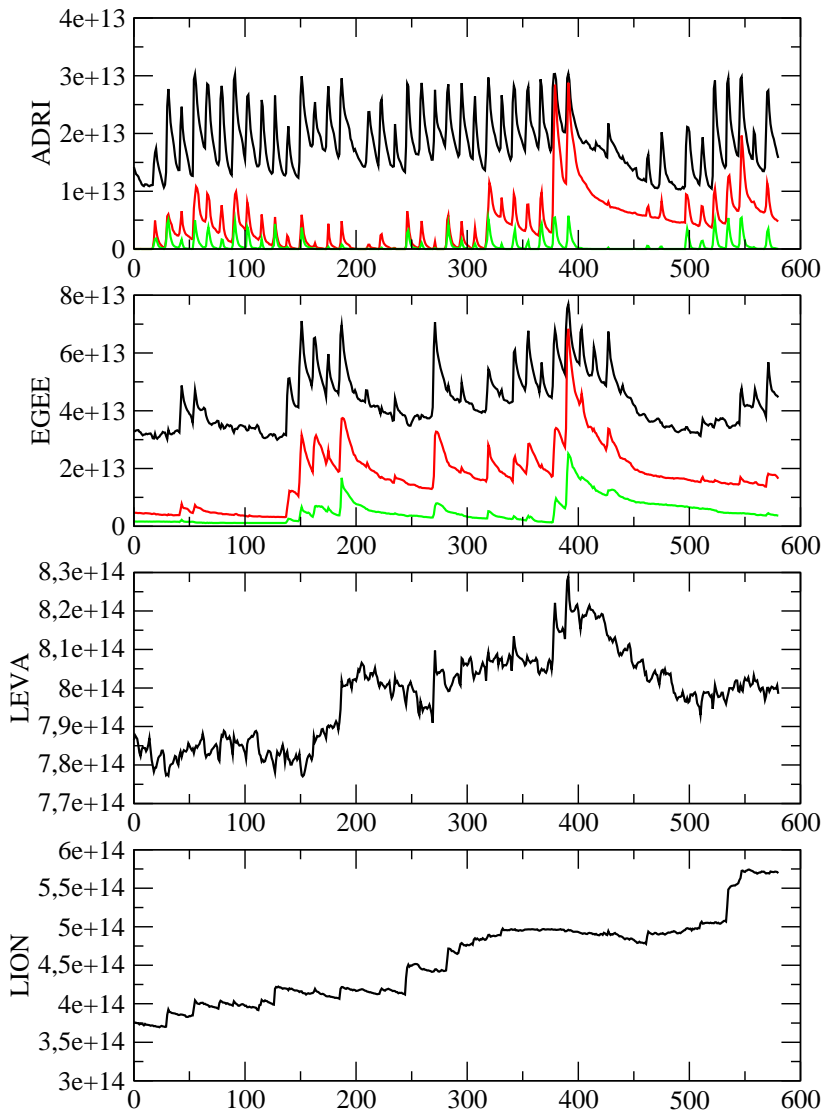


Figure 32: Monthly volume of water in m^3 with density greater than 29.1 (black), 29.2 (red) and 29.3 (green) for the Adriatic Sea (ADRI), Aegean Sea (EGEE), Levantine basin (LEVA) and the Gulf of Lions (LION).

3.8 Water, heat and salt budgets

Table 5 shows the different components computed on the 1961-2008 period for the whole Mediterranean basin.

Budget component	1961-2008 Mean (standard deviation)
Water inflow at Gibraltar	0.86 Sv (0.03)
Water outflow at Gibraltar	-0.81 Sv (0.03)
Net water transport at Gibraltar	0.05 Sv (0.01) or 0.68 m/yr (0.06)
Water flux through the surface	0.68 m/yr (0.06)
Heat flux through the surface	-4.6 W/m ² (4.2)
Heat transport at Gibraltar	5.5 W/m ² (0.6)
Heat content trend	0.003 K/yr or 0.7 W/m ²
Salt transport at Gibraltar	4.5.10 ¹⁵ g/yr
Mediterranean salt content trend	5.3.10 ¹⁵ g/yr

Table 5: Mean and standard deviation of the water, heat and salt budgets.

4 Conclusion

We have shown in this document some results of a 1961-2008 simulation of the Mediterranean Sea with the NEMOMED8 oceanic model. In general it is a quite realistic simulation, and the comparisons with the observations show that the chronology is correct and the thermohaline circulation well represented considering the 10 km horizontal resolution of the model. It will be continued as soon as the surface fluxes are available.

It also shows that the ARPEGE-Climate surface fluxes as they are produced with the dynamical downscaling of ERA40 are appropriate for this kind of hindcast. The next step may be the production of these fluxes with another bulk formula in the atmospheric model, ECUME, and/or at a higher resolution, with ALADIN-Climate for example. Then the same hindcast of the Mediterranean Sea could be produced with the NEMOMED12 model.

5 Acknowledgments

S. Somot, J. Beuvier, M. Déqué, in Météo-France/CNRM, have helped for the set-up of this simulation. We acknowledge P. Rogel, N. Daget, W. Ludwig, E. Stanev and M. Rixen for giving us their data.

Special thanks to the people who use this simulation and give their comments and propositions of improvements for the next ones.

6 References

Beuvier, J., F. Sevault, M. Herrmann, H. Kontoyiannis, W. Ludwig, M. Rixen, E. Stanev, K. Beranger, and S. Somot, 2010 : Modelling the Mediterranean Sea interannual variability during 1961-2000 : focus on the Eastern Mediterranean Transient, *J. Geophys. Res.*, 115, C08017, doi:10.1029/2009JC005950.

Daget, N., A. T. Weaver, and M. A. Balmaseda, 2009: Ensemble estimation of background-errors variances in a three-dimensional variational data assimilation system for the global ocean, *Quarterly Journal of the Royal Meteorological Society*, 135, 1071-1094.

Déqué, M. and J.-P. Piedelievre, 1995: High resolution climate simulation over Europe, *Climate dynamics*, 11, 321-339.

Herrmann, M., F. Sevault, J. Beuvier, S. Somot, 2010: What induced the exceptional 2005 convection event in the Northwestern Mediterranean basin? Answers from a modeling study. Submitted to *JGR*.

Ludwig, W., E. Dumont, M. Meybeck, and S. Heussner, 2009: River discharges of water and nutrients to the Mediterranean and Black Sea: Major drivers for ecosystem changes during past and future decades?, *Progress in Oceanography*, 80, 199-217.

- Mertens, C. and F. Schott, 1998: Interannual variability of deep-water formation in the Northwestern Mediterranean, *J. Phys. Oceanography*, 28, 1410-1424.
- Reynaud, T., P. Legrand, H. Mercier, B. Barnier, 1998: A new analysis of hydrographic data in the Atlantic and its application to an inverse modeling study. *International WOCE Newsletters*, 32,29-31.
- Rixen, M. et al., 2005: The Western Mediterranean Deep Water: a proxy for climate change, *Geophys. Res. Lett.*, 32, L12608, doi:10.1029/2005GL022702.
- Sevault, F., S. Somot, and J. Beuvier, 2009: A regional version of the NEMO ocean engine on the Mediterranean Sea: NEMOMED8 user's guide. Note de centre n°107, GMGEC, CNRM, Toulouse, France, mai 2009.
- Simmons, A., and J. Gibson, 2000: The ERA40 project plan, ERA40 Project Report Series n°1, ECMWF, Reading, United Kingdom.
- Stanev, E. V., P.-Y. Le Traon, and E. L. Peneva, 2000: Sea level variations and their dependancy on meteorological and hydrological forcings: Analysis of altimeter and surface data for the Black Sea, *Journal of Geophysical Research*, 105 (C7), 17, 203-216.
- Stanev, E. V., and E. L. Peneva, 2002: Regional sea level response to global climatic change: Black Sea examples, *Global and Planetary Changes*, 32, 33-47.
- Valcke, S., 2006: OASIS User guide, prism_2-5, PRISM-Support Initiative, Report n°3, CERFACS TR/CMGC/063/73, September 2006.
- Vörösmarty, C., B. Fekete, and B. Tucker, 1996: Global river discharge database, RivDis, UNESCO, Paris, International Hydrological Program, Global Hydrological Archive and Analysis Systems. References